Exp. Eye Res. (2001) **73**, 851–858
doi:10.1006/exer.2001.1089, available online at http://www.idealibrary.com on IDEAL®

Measurement of TIMP-3 Expression and Bruch's Membrane Thickness in Human Macula

TRACEY A. BAILEY*, ROBERT A. ALEXANDER, SANDER R. DUBOVY, PHILIP J. LUTHERT AND N. H. VICTOR CHONG

Department of Pathology, Institute of Ophthalmology, UCL, Bath Street, London EC1V 9EL, U.K.

(*Received St. Louis 8 May 2001 and accepted in revised form 16 August 2001*)

An increase or accumulation in tissue inhibitor of matrix metalloproteinases-3 (TIMP-3) protein in Bruch's membrane with ageing in normal eyes, and in age related macular degeneration (AMD) has been previously demonstrated. The purpose of this study was to determine whether the expression of TIMP-3 mRNA increases with age, and to define any relationship between altered expression and Bruch's membrane thickness. Normal eyes were obtained from 30 donors (age range 15–90 years). Full-thickness 8 mm macular punches centred on the fovea were taken to allow removal of the chorioretinal complex, for subsequent nucleic acid extraction. Samples were normalized for RNA degradation using beta-actin reverse transcriptase–polymerase chain reaction (RT–PCR). A competitive RT–PCR was then used to allow measurement of TIMP-3 gene expression in each sample. The tissue adjacent to that used for nucleic acid extraction was processed histologically to allow determination of Bruch's membrane thickness. Bruch's membrane thickness was found to increase with age ($P < 0{\cdot}01$), but TIMP-3 expression, as measured by competitive RT–PCR, was not significantly increased with age ($P = 0{\cdot}19$). An inverse correlation was noted between TIMP-3 expression and Bruch's membrane thickness after controlling for age ($P = 0{\cdot}032$). The results of this study suggest that TIMP-3 expression does not alter significantly with age. Therefore, accumulation of the TIMP-3 protein must occur by a mechanism other than increased expression. TIMP-3 protein levels may still prove to contribute to events associated with ageing in the macula, such as matrix remodelling in Bruch's membrane. Further studies are required to elucidate the precise interactions and turnover of the TIMP-3 protein, and resulting changes in the control of matrix metalloproteinase activity in the ageing macula.

Key words: age related macular degeneration; Bruch's membrane; extracellular matrix; TIMP-3; gene expression; metalloproteinases; retinal pigment epithelium.

1. Introduction

Age related macular degeneration (AMD) is the most common cause of blindness in developed countries (Evans and Wormald, 1996). Since age is the dominant risk factor for AMD, it is important to characterize molecular events of the normal ageing process so that those of potential relevance to AMD may be identified.

AMD is characterized by the presence of macular drusen, abnormal pigmentation of the retinal pigment epithelium (RPE), geographic atrophy and choroidal neovascularization (Bird et al., 1995). The clinical and pathological features of AMD are in many ways similar to Sorsby's fundus dystrophy (SFD), an early onset, autosomal dominant condition. This disease is linked to mutations of the tissue inhibitor of metalloproteinase 3 (TIMP-3) locus (Weber et al., 1994; Felbor et al., 1995; Jacobson, Cideciyan and Regunath, 1995; Langton et al., 2000). SFD mutations result in a substitution that causes incorporation of an additional cysteine residue and hence inappropriate disulphide bridge formation. The most common SFD mutation is thought to cause formation of a TIMP-3 dimer, which may be resistant to normal mechanisms of turnover (Langton, Barker and McKie, 1998), and lead to the abnormal accumulation of TIMP-3 demonstrated by immunohistochemistry (Fariss et al., 1997; Chong et al., 2000). This mutant protein retains its ability to bind to the extracellular matrix (ECM) and inhibit metalloproteinases (Langton et al., 1998), hence its contribution to the pathogenesis of the disease is presumably via a mechanism other than loss of function. Possibilities include the induction of RPE apoptosis by increased TIMP-3 levels as suggested by experiments in a colon carcinoma cell line (Bian et al., 1996; Smith et al., 1997), or more simply by contributing to the thickening of Bruch's membrane where the dimer accumulates and blocks the nutrient path to the retina. Because of the similarities between AMD and SFD, a role for TIMP-3 in AMD has been investigated, although mutation has already been ruled out as a causative factor (De La Paz et al., 1997; Felbor et al., 1997).

In the normal eye, TIMP-3 protein locates to Bruch's membrane (Fariss et al., 1997; Chong et al., 2000), with transcript production localizing mainly to the RPE and choroids (Ruiz, Brett and Bok, 1996; Vranka

* Address correspondence to: Tracey A. Bailey, Department of Pathology, Institute of Ophthalmology, UCL, Bath Street, London EC1V 9EL, U.K. E-mail: tracey.bailey@ucl.ac.uk

0014-4835/01/120851+08 $35.00/0

et al., 1997). Western blot analysis and reverse zymography have been used to show an increase in TIMP-3 with normal ageing (Kamei and Hollyfield, 1999). An accumulation of the TIMP-3 protein in the Bruch's membrane of AMD eyes has been demonstrated by immunohistochemistry (Fariss et al., 1997), and a similar accumulation has been observed in SFD (Fariss et al., 1998; Chong et al., 2000). Thickening of the Bruch's membrane occurs as part of normal ageing (Sarks, 1976; Newsome, Huh and Green 1987; Van der Schaft et al., 1992; Okubo et al., 1999), so it may be argued that the accumulation of TIMP-3 is associated with an overall increase in the deposition of matrix proteins in this layer, or alternatively causes decreased turnover of matrix proteins via the increased inhibition of metalloproteinases.

We investigated whether the increase of TIMP-3 protein in ageing is due to increased TIMP-3 gene expression, and the nature of the relationship between expression and Bruch's membrane thickness.

2. Methods

Tissue Preparation

Eyes were obtained from Moorfields Eye Bank from normal donors with informed consent for research use. If both eyes from the same donor were available, only one eye was used for this study. Storage until receipt from the eye bank was at 4°C. The anterior segment of each eye was removed. Gross examination was performed under a dissecting microscope. Any case with visible macular pathology was excluded from the study. An 8 mm macular punch centred on the fovea was taken from one eye of each of the donors. This punch was either processed immediately or stored at −80°C until required. The sclera was removed, then the whole chorioretinal complex was used for nucleic acid extraction, to facilitate tissue handling and subsequent RNA quantification. The remaining tissue was then fixed in formaldehyde. Fixed posterior segments were trimmed, orientated and processed so that paraffin sections could be cut perpendicular to the Bruch's membrane for thickness measurement. Paraffin sections were also used to exclude cases of AMD from the study, since clinical histories were not available.

Bruch's Membrane Thickness Measurement

Five micron thick sections were cut from each eye and stained by the periodic acid Schiff (PAS) procedure. These were photographed on a Leica RBE light microscope (Leica, Wetzlar, Germany) using a × 40 objective with identical settings. A microscope slide graticule was photographed on numerous occasions to aid measurement reproducibility.

The photographic images were digitized using Nikon Coolscan slide scanner (Nikon U.K. Ltd, Kingston-upon-Thames, U.K.). A grid was placed over the images using Abode Photoshop (Abode Systems Inc., San Jose, U.S.A.), and measurements were taken adjacent to the gridlines crossing the Bruch's membrane. Light microscopic Bruch's membrane thickness was defined by the extent of the PAS staining and was measured by the number of pixels using Abode Photoshop measuring tool. A total of 15 measurements were taken for each donor.

Two observers masked to the age of the donor and the reverse transcriptase–polymerase chain reaction (RT–PCR) results carried out the Bruch's membrane thickness measurement. A number of images were measured more than once by the same observer in different sessions. Inter-observer and intra-observer differences analysis were performed by the Student's *t*-test. The mean measurement of the two observers was used for further statistical analysis.

Nucleic Acid Extraction and Equalization of Samples

Total RNA was extracted from the chorioretinal complex using a Qiagen RNeasy® Mini kit (Qiagen, Crawley, U.K.) according to the manufacturer's protocol. The flow-through for each step was retained for back-extraction of genomic DNA by phenol–chloroform extraction and ethanol precipitation. The resulting RNA and DNA from these procedures was quantified by optical density at 260 nm.

Because of a wide variation in post-mortem intervals (PMIs), the quality of messenger RNA (mRNA) was subsequently checked by RT–PCR with beta-actin primers and standard reaction conditions (Table I). This reaction was designed to be semi-quantitative by stopping PCR in the exponential phase to compare product levels (23 cycles for this reaction), so equalized levels of message could be utilized in the quantitation of TIMP-3 message.

Exclusion of SFD by PCR and Restriction Analysis

None of the donors were known to have a history of SFD, but as an exclusion procedure, genomic DNA was used in PCR with primers designed to amplify exon 5 of the TIMP-3 gene and give a 243 base pair product (Table I). This product was digested with the restriction enzyme *NsiI* (Promega, Madison, U.S.A.), using conditions recommended by the manufacturer, since the site for this enzyme is introduced by the common mutation for SFD (Weber et al., 1994). The digested and undigested products were then compared by agarose gel electrophoresis, with mutated DNA giving bands of 208 and 35 base pairs. Genomic DNA extracted from the blood of a known SFD patient with the Ser181Cys mutation in TIMP-3 was used as a positive control.

TABLE I

Primers used for competitor construction, mutation detection and competitive RT–PCR

Primer pair function	Sequences	Product size
Competitor Construction	Forward (T7 promoter sequence underlined): 5′-TAA TAC GAC TCA CTA TAG GGC CAT CAA GCA GAT GAA GAT G-3′ Reverse (2nd and 1st R-primer sites separated by/): 5′-TCA TAG ACG CGA CCT GTC AG/G TAG CAG GAC TTG ATC TTG C-3′	182 bp
TIMP-3 Exon 5 Primers for subsequent restriction analysis	Forward: 5′- GTC CAT CAA CTG CTG CCT G-3′ Reverse: 5′-AGG GTC TGG CGC TCA GGG-3′	243 bp
TIMP-3 RT–PCR to distinguish between donor message and competitor	Forward: 5′-CCA TCA AGC AGA TGA AGA TGT ACC-3′ Reverse: 5′-GGT AGT AGC AGG ACT TGA TCT TCC-3′	271 bp or 162 bp

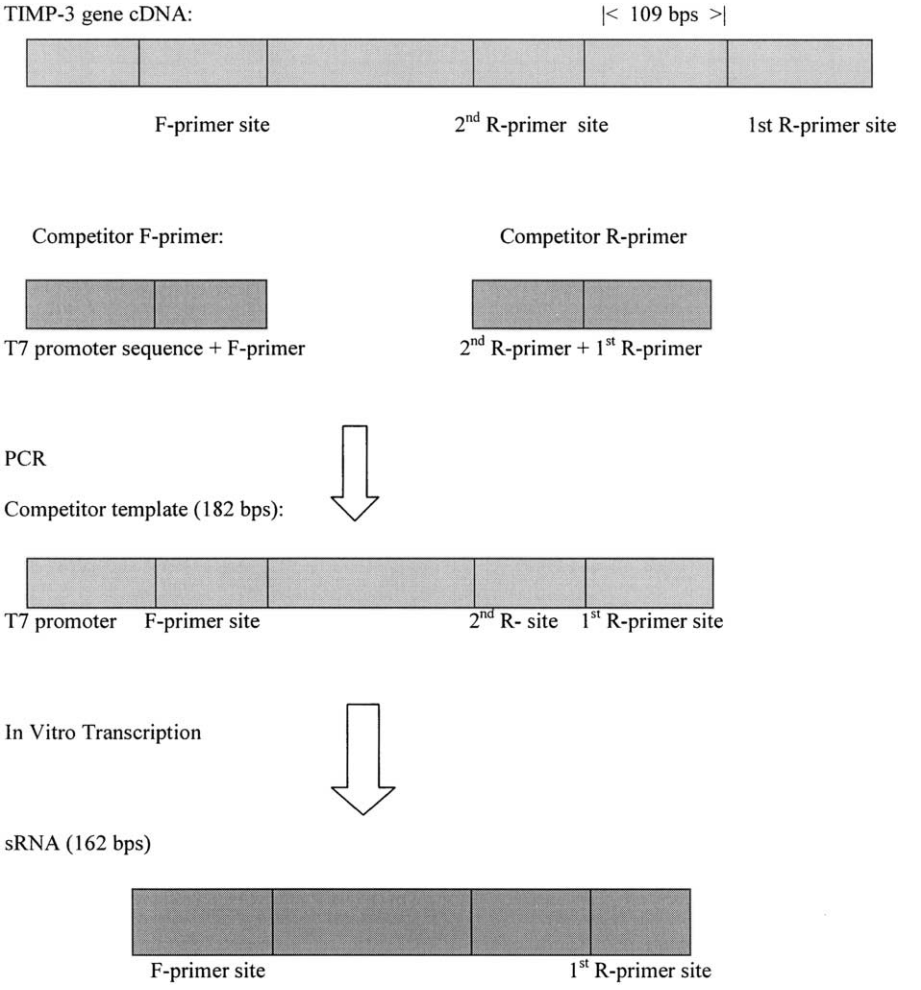

FIG. 1. Construction of a synthetic RNA competitor for use in RT–PCR. This demonstrates how primer sites in the target are combined in the competitor template to allow RNA synthesis via use of the T7 promoter sequence. The resulting transcript is 109 base pairs shorter than the target in the donor sample, yet otherwise shares the same sequence.

Synthesis of an RNA Competitor (sRNA)

The competitor in this assay was synthesized from a PCR product sharing the same primer binding sites as the target RNA transcript, but produced in such a way that the synthetic competitor was 109 bases shorter to allow distinction of the different products by agarose gel electrophoresis (Fig. 1). This was achieved by the reverse transcription of 1 μg of total human kidney RNA (Invitrogen, Groningen, The Netherlands), as the kidney is a rich expresser of TIMP-3 (Zeng et al., 1998). The resulting copy DNA (cDNA) was then amplified by PCR using a forward primer, the same as that to be used in the quantitative reaction (Sequences from Kenney et al., 1998), but with a T7 promoter sequence tagged to the 5′ end (Table I). The reverse primer consisted of the reverse sequence to be used in

the quantitative reaction, plus sequence downstream of this site to 'cut out' approximately 100 bases (Table I). In all the instances, primers were synthesized by Amersham Pharmacia Biotech (Little Chalfont, U.K.). This method is essentially the same as that used by Zhang et al. (1997).

After PCR, the size of the product was checked by agarose gel electrophoresis. A band of 182 base pairs corresponded to the template for sRNA synthesis plus the T7 promoter sequence. This PCR product was then used in an in vitro transcription (IVT) reaction to produce the competitor RNA. Purification of the PCR prior to IVT requires dilution of 30 μl of the PCR product in 0·5 ml TE buffer, followed by two phenol–chloroform extractions with retention of the aqueous layer, and then ethanol precipitation. The purified DNA was then added to DTT (10 mM), rNTPs (0·5 mM), 1 × T7 RNA polymerase buffer, 1 U μl^{-1} RNasin, 1 U μl^{-1} T7 RNA polymerase and 1·25 μM T7 primer (all supplied by Promega, Madison, U.S.A.) in a total volume of 20 μl. The RNA was then synthesized during incubation at 37°C for 1 hr.

Synthetic standard RNA (sRNA) was extracted from the reaction mixture using the RNeasy® kit (Qiagen, Crawley, U.K.). This was used according to the manufacturer's instructions for 'RNA clean-up', incorporating a DNase step while the RNA is membrane bound. The concentration of the sRNA was subsequently quantified by UV spectrophotometry, and this was used to calculate the 'copy number' with the predicted molecular weight.

Optimization of Quantitative Competitive RT–PCR

Optimization of cycle number with constant RNA was required to ensure that quantitative reactions were stopped in the exponential phase of PCR. This was efeected in a similar manner to that use by Zhang et al. (1997). Variation of RNA levels was also required to determine the detection limit of the assay. Master mixes of reagents were employed wherever possible to reduce tube to tube variation.

The detection limits of the digital system and agarose gel electrophoresis were assessed by using a single banded PCR product and running it and successive one in two dilutions of the product. The log of the mean intensity of each band was then plotted against the log of the volume of PCR product in each lane. Values not conforming to a linear plot under these circumstances were excluded from the range of intensities used for subsequent calculations.

Quantitative Competitive RT–PCR with RNA Extracted from Donor Eyes

Once optimized, the RT–PCR protocol was used to perform at least five reactions per donor sample. Each reaction contained a constant amount of total RNA from the donor (usually 50 or 100 ng, depending on extraction yield and adjusted if necessary after beta-actin RT–PCR), plus a set amount of the competitor RNA (between 0·01 and 10 pg). The competitor RNA was calculated to consist of $6{\cdot}2 \times 10^3$ copies of sequence per picogram. RT–PCR was carried out using basic conditions recommended by Promega using their reverse transcription system, but variation caused by pipeting error minimized by the use of master mixes. These master mixes were then combined to create 10 μl reactions with the varying competitor concentrations for each donor, and overlaid with mineral oil (Sigma-Aldrich, Poole, U.K.). After reverse transcription under conditions described previously, 40 μl of a PCR master mix was added to each tube comprising $MgCl_2$, 10 × buffer, Taq polymerase and forward and reverse primers. PCR was then performed for 23 cycles at 94°C for 30 sec, 60°C for 30 sec, and 72°C for 30 sec, followed by a final extension of 3 min at 72°C. Products had previously been found to be acquired during the exponential phase of the reaction at 23 cycles.

Quantification of RT–PCR Products

RT–PCR products were analysed in a 2 % w/v agarose gel. The bands were photographed on a UV light box (UVP, Upland, U.S.A.) using a DC120 Zoom digital camera (Kodak, Rochester, U.S.A.), and then quantified using the digital science program (Kodak, Rochester, U.S.A.). The 'mean intensity' parameter was utilized to account for both intensity and area of each band.

For each band, a target RNA to competitor RNA intensity ratio was obtained. Since the amount of competitor RNA added to the reaction was known, the amount of target RNA could therefore be calculated and given as a value of copy number per ng total RNA. In each assay, the copy number for a control RNA (total RNA from normal human kidney) was calculated. To correct for inter-assay variation, the TIMP-3 value for each donor is given relative to the copy number for the control RNA (as previously described by Ozaki et al., 1999).

Statistical Analysis

PMI was compared to the RNA yield and TIMP-3 values to ensure that delay in tissue processing had been corrected for by the methodology.

Linear regression and partial correlation correction coefficients of age, Bruch's membrane thickness and TIMP-3 expression were performed using SPSS statistical software (SPSS Inc., Chicago, U.S.A.).

3. Results

Thity eyes from 30 donors were used in this study. The mean age was 65·1 years (range 15–90). Details of age, PMI, sex and cause of death are shown in

TABLE II

Donor details

Donor number	Age of death (years)	PMI (hr)	Sex	Cause of death if known
1	15	48	F	Mega hyaluronic acidaemia
2	21	35	M	Road traffic accident
3	27	39	F	Meningitis
4	41	48	M	Cardiac illness
5	43	82	F	Breast cancer
6	49	36	F	No record
7	50	44	F	Breast cancer
8	52	42	F	Subarachnoid haematoma
9	55	45	M	Brain tumour
10	55	54	F	Bowel cancer
11	57	48	M	Bladder cancer
12	58	24	F	Stomach cancer
13	59	65	M	Pancreatic cancer
14	59	26	F	Intra-cranial haemorrhage
15	61	29	M	Prostate cancer
16	63	29	F	Myocardial infarction
17	64	24	M	Respiratory disease
18	67	38	M	Mesothelioma
19	68	49	M	Prostate cancer
20	72	22	F	Subarachnoid haematoma
21	74	48	F	Ovarian cancer
22	75	70	M	Cardiac illness
23	75	48	F	Lung cancer
24	76	58	M	Astrocytoma
25	79	72	F	Pulmonary embolism
26	79	24	M	Respiratory infection
27	83	40	F	No record
28	88	36	M	Ruptured aortic aneurysm
29	88	51	F	Myocardial infarction
30	90	48	F	Cardiac failure

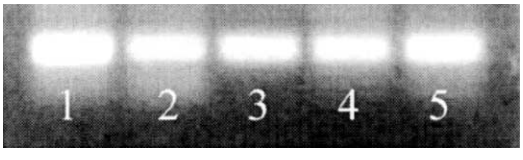

FIG. 2. An agarose gel demonstrating products of a semi-quantitative beta-actin RT–PCR from 100 ng total RNA obtained after varying PMIs: Lane 1, control RNA (human kidney total RNA); lane 2, donor RNA 24 hr PMI; lane 3, donor RNA 34 hr PMI; lane 4, donor RNA 38 hr PMI; lane 5, donor RNA 48 hr PMI. Digital analysis of this gel revealed the mean band intensities to vary less than 2 % between donor samples. Donor band intensities in this instance were approximately 8 % less than the control, so total RNA levels required only slight adjustment before quantitative competitive RT–PCR for TIMP-3.

Table II. RNA and DNA were extracted from all the cases. No relationship was found between the PMI and RNA yield. No donors were found to carry the common mutation in the TIMP-3 gene as demonstrated by *NsiI* restriction analysis (results not shown). All samples were equalized for beta-actin expression prior to analysis of TIMP-3 expression (Fig. 2).

Fig. 4 presents the results as a graph of TIMP-3 expression value vs donor age [Fig. 4(A)], and Bruch's membrane thickness vs donor age [Fig. 4(B)].

The mean inter-observer difference for the Bruch's membrane measurement was less than 10 % and it was statistically insignificant. The mean intra-observer difference was less than 4 % and it was statistically insignificant.

The Bruch's membrane thickness was statistically significantly increased with age ($P = 0{\cdot}001$) but the TIMP-3 expression was not significantly increased with age ($P = 0{\cdot}189$) [Fig. 4(A) and (B)]. TIMP-3 expression was inversely correlated with Bruch's membrane thickness, using partial correlation coefficient analysis, after controlling for age ($P = 0{\cdot}032$).

4. Discussion

TIMP-3 inhibits metalloproteinase activities. As it is the main TIMP in Bruch's membrane (Fariss et al., 1997), it is believed to play a significant role in the extracellular matrix turnover in this layer. The gelatinases are one class of MMPs that have been investigated with respect to ocular ageing and AMD (reviewed in Sethi et al., 2000). MMP-2 (gelatinase A) and -9 (elatinase B) are both present in the Bruch's–choroid complex, and although MMP-9 predominates, the levels of both proteins have been shown to increase with age (Guo, Hussain and Limb, 1999). Most

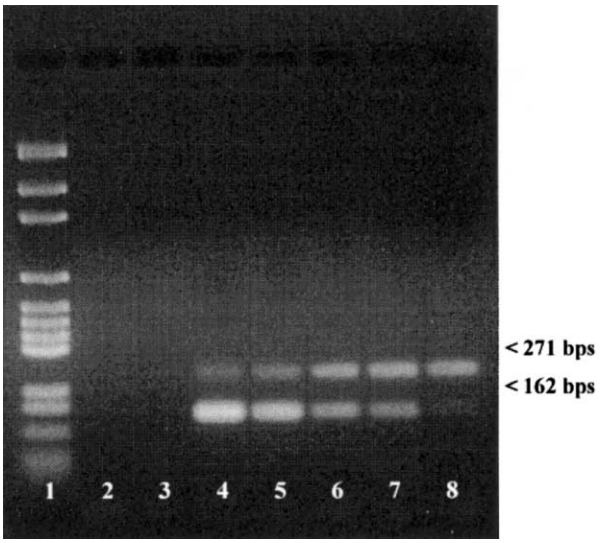

FIG. 3. An agarose gel demonstrating visualization of products from donor sample and competitor for use in quantifying TIMP-3: Lane 1, pGem marker (Promega); lane 2, no template control; lane 3, no reverse transcription control; lanes 4–8 show RT–PCR products from 100 ng total human kidney RNA (Invitrogen) plus (4) 1 pg competitor, (5) 0·5 pg competitor, (6) 0·1 pg competitor, (7) 0·05 pg competitor and (8) 0·01 pg competitor. With decreasing amounts of the synthetic RNA competitor, the amount of product from the total RNA is seen to increase, and the ratio between the band intensities can then be used to calculate TIMP-3 copy number in the total RNA sample.

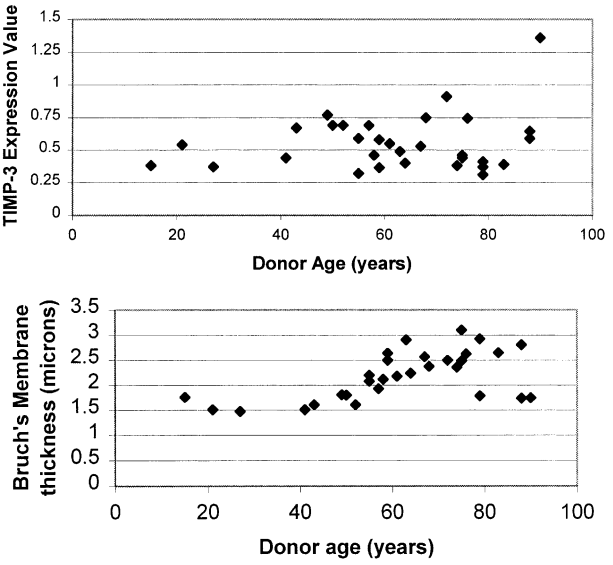

FIG. 4. (A) Mean TIMP-3 expression and Bruch's membrane thickness vs age of donor, $P = 0{\cdot}189$; (B) mean Bruch's membrane thickness vs age of donor, $P < 0{\cdot}01$.

previous studies have concentrated on the measurement of protein levels. TIMP-3 was investigated at the level of RNA transcript production by the development of a quantitative competitive RT–PCR, for use with RNA extracted from the chorioretinal complex.

Ideally, RNA would be extracted from eyes with the shortest possible post mortem delay. Although most of the samples were obtained in less than 48 hr of post mortem, the precise delay time was beyond our control and varied from 22 to 82 hr. However, it was felt that there was justification in the continuation of this work with this methodology being designed to correct for these variations. In a previous study, total cellular RNAs were degraded to varying extents by Tong et al. (1997), who then used RT–PCR of the housekeeping gene GAPDH to normalize samples prior to the measurement of expression of other genes. Data from this group suggested that every specific mRNA analysed degraded to a similar extent, and therefore normalization could be used to correct relative mRNA quantitation in degraded samples. It was also noted that amplicon length may influence quantitation, since longer transcripts will be less abundant in degraded samples, so target length for both the beta-actin and TIMP-3 RT–PCR reactions were kept below 300 bp in this study. Similarly, a study on brain tissue found levels of five specific transcripts, including GAPDH and beta-actin to be stable when the interval between death and freezing of the tissue was up to 4 days (Schramm et al., 1999). Despite debate by others regarding how long after death reliable analysis of RNA can be made, it was decided to proceed with this investigation, which otherwise would have been impossible due to difficulties with supply of donor tissue in the U.K. In support of this decision, levels of total RNA and TIMP-3 value were not found to show any correlation with post mortem time (data not shown).

After normalization of samples, the results of this study provide no evidence to suggest that the previously reported accumulation in TIMP-3 in Bruch's membrane with age is due to increased gene expression. It would have been desirable to quantify the TIMP-3 protein in these donors, but low extraction yield of RNA and high use of that RNA in the RT–PCR meant all macular tissue was used from most donors. Despite the lack of data relating to protein levels, it is suggested that the observed increase in TIMP-3 with age in other studies could be due to a defect in the turnover of the protein, leading to sustained MMP inhibition and thus Bruch's membrane thickening. This has already been suggested by Langton et al. (2000) as a possible mode of pathogenesis in SFD. Although in SFD this seems likely to be due to dimerization of the mutant protein, this is less likely to be the case in ageing or AMD.

Thickening of the Bruch's membrane with age was demonstrated for this set of donors, as previously shown by the study of another set of donors (Okubo et al., 1999). Bruch's membrane thickness was measured on the cut edge of the macular punch, which is just beyond the vascular arcade and might be considered to be just beyond the anatomical macula. Nonetheless, it is very close to the macula and indeed the measurements are similar to the previous study of

the Bruch's membrane thickness in the macular region (Okubo et al., 1999). As the other eye is not always available, allowing for the limitation, the method used allowed specimen consistency for direct comparison between donors.

When adjusted for age, TIMP-3 expression was found to be inversely correlated to the Bruch's membrane thickness. This would seem to oppose the idea that increased TIMP-3 leads to increased MMP inhibition, and thus thickened Bruch's membrane. One hypothesis of why higher TIMP-3 expression is associated with a thinner Bruch's membrane is that TIMP-3 induces further production of MMPs and an imbalance has caused matrix turnover to be increased. MMP-2 and -9 have indeed been shown to increase in ageing and AMD (Guo et al., 1999), but this has not been related to the Bruch's membrane thickness in any study to date. Another possibility is that expression is elevated as a response to a thinner Bruch's membrane, and conversely low TIMP-3 expression is a response to a thickened membrane in an attempt to rectify the situation. As well as thickening with age, Bruch's membrane also becomes more disorganized such that individual layers are harder to discern. Eagle (1984) suggested that this was due to a generalized deregulation of matrix deposition and turnover, and decreased TIMP-3 turnover, in turn affecting metalloproteinase activity, could well be part of this multifactorial process. It would therefore be desirable to take a multifactorial approach to analyse such changes, as has already been attempted by Hageman (2000). Since the inner layer of Bruch's membrane generally changes first, the RPE is implicated as the source of changes and currently provides the main line of investigation.

An important factor to ascertain with respect to TIMP-3 in the ageing eye is whether or not the accumulated protein is truly functional. Although other studies have used reverse gelatin zymography to claim that accumulated protein retains inhibitory activity, it is not certain how representative this assay is of the situation in vivo. Since proteins are effectively separated by SDS–PAGE, associations with other factors may be lost, and it could be that, in the ageing eye, TIMP-3 is binding an additional protein unrelated to metalloproteinases, which could be not only preventing TIMP-3 turnover, but also preventing its inhibitory function. Langton et al. (2000) have already suggested that the mechanism of TIMP-3 accumulation may be due to the increased binding by products of advanced protein glycosylation (AGES), which accumulate with ageing. Evidence to support this hypothesis includes the presence of such products in the Bruch's membrane (Farboud et al., 1999). It is interesting to note that these products can induce cross-linking of collagen (Sajithlal et al., 1998), a probable component of basal laminar deposits found in ageing and AMD. Another perhaps relevant finding is that cell activation in response to AGE-modified proteins is associated with increased expression of extracellular matrix proteins, and can also be associated with angiogenesis, oxidative stress and programmed cell death, which have all been implicated in contributing to AMD (Tezuka et al., 1993; Yan et al., 1994; Yamagishi et al., 1996).

This study suggests TIMP-3/MMPs expression of RPE cells in response to various stimuli that may be relevant to the ageing process and pathogenesis of AMD. This requires further clarification. Furthermore, Bruch's membrane thickness may be a therapeutic target for modification in the early stages of age related maculopathy.

Acknowledgements

The authors would like to thank Moorfields Eye Bank for provision of donor material. This research was supported by a Royal College of Surgeons of Edinburgh research grant.

References

Bian, J., Wang, Y., Smith, M. R., Kim, H., Jacobs, C., Jackman, J., Kung, H. F., Colburn, N. H. and Sun, Y. (1996). Suppression of in vivo tumor growth and induction of suspension cell death by tissue inhibitor of metalloproteinases (TIMP)-3. *Carcinogenesis* **17**, 1805–11.

Bird, A. C., Bressler, N. M., Bressler, S. B., Chisholm, I. H., Coscas, G., Davis, M. D., de Jong, P. T., Klaver, C. C., Klein, B. E. and Klein, R. (1995). The International ARM Epidemiological Study Group. An international classification and grading system for age related maculopathy and age related macular degeneration. *Surv. Ophthalmol.* **39**, 367–74.

Chong, N. H. V., Alexander, R. A., Gin, T., Bird, A. C. and Luthert, P. J. (2000). TIMP-3, Collagen and elastin immunohistochemistry and histopathology of Sorsby's fundus dystrophy. *Invest. Ophthalmol. Vis. Sci.* **41**, 898–902.

De La Paz, M. A., Pericak-Vance, M. A., Lennon, F. and Seddon, J. M. (1997). Exclusion of TIMP-3 as a candidate locus in age related macular degeneration. *Invest. Ophthalmol. Vis. Sci.* **38**, 1060–65.

Eagle, R. C., Jr (1984). Mechanisms of maculopathy. *Ophthalmology* **91**, 613–25.

Evans, J. and Wormald, R. (1996). Is the incidence of registerable age-related macular degeneration increasing? *Br. J. Ophthalmol.* **80**, 2.

Farboud, B., Aotaki-Keen, A., Miyata, T., Hjelmeland, L. M. and Handa, J. T. (1999). Development of a polyclonal antibody with broad epitope specificity for advanced glycation endproducts and localization of these epitopes in Bruch's membrane of the ageing eye. *Mol. Vis.* **5**, 11.

Fariss, R. N., Apte, S. S., Luthert, P. J., Bird, A. C. and Milam, A. H. (1998). Accumulation of tissue inhibitor of metalloproteinases-3 in human eyes with Sorsby's fundus dystrophy or retinitis pigmentosa. *Br. J. Ophthalmol.* **82**, 1329–34.

Fariss, R. N., Apte, S. S., Olsen, B. R., Milam, A. H. and Iwata, K. (1997). Tissue inhibitor of metalloproteinase is a component of Bruch's membrane of the eye. *Am. J. Pathol.* **150**, 323–8.

Felbor, U., Doepner, D., Schneider, U., Zrenner, E. and Weber, B. H. (1997). Evaluation of the gene encoding

the tissue inhibitor of metalloproteinases-3 in various maculopathies. *Invest. Ophthalmol. Vis. Sci.* **38**, 1054–9.

Felbor, U., Stohr, H., Amann, T., Schonherr, U. and Weber, B. H. F. (1995). A novel Ser156Cys mutation in the tissue inhibitor of metalloproteinase-3 (TIMP-3) in Sorsby's fundus dystrophy with unusual clinical features. *Hum. Mol. Genet.* **4**, 2415–6.

Guo, L., Hussain, A. A. and Limb, G. A. (1999). Age-dependent variation in metalloproteinase activity of isolated human Bruch's membrane and choroid. *Invest. Ophthalmol. Vis. Sci.* **40**, 2676–82.

Hageman, G. (2000). Toward the characterization of pathways involved in the etiology of age related macular degeneration: a strategy based upon the use of human donor eyes, proteomics and gene array analysis [ARVO symposium]. *Invest. Ophthalmol. Vis. Sci.* **41**(4): 14.

Jacobson, S. G., Cideciyan, A. V. and Regunath, G. (1995). Night blindness in Sorsby's fundus dystrophy reversed by Vitamin A. *Nat. Genet.* **11**, 27–32.

Kamei, M. and Hollyfield, J. G. (1999). TIMP-3 in Bruch's membrane: changes during ageing and age related macular degeneration. *Invest. Ophthalmol. Vis. Sci.* **40**, 2367–75.

Kenney, M. C., Chwa, M., Alba, A., Saghizadeh, M., Huang, Z. S. and Brown, D. J. (1998). Localization of TIMP-1, TIMP-2, TIMP-3, gelatinase A and gelatinase B in pathological human corneas. *Curr. Eye Res.* **17**, 238–46.

Langton, K. P., Barker, M. D. and McKie, N. (1998). Localization of the functional domains of human tissue inhibitor of metalloproteinases-3 and the effects of a Sorsby's fundus dystrophy mutation. *J. Biol. Chem.* **273**, 16779–81.

Langton, K. P., McKie, N., Curtis, A., Goodship, J. A., Bond, P. M., Barker, M. D. and Clarke, M. A. (2000). A novel TIMP-3 mutaion reveals a common molecular phenotype in Sorsby's fundus dystrophy. *J. Biol. Chem.* **275**, 27027–31.

Newsome, D. A., Huh, W. and Green, W. R. (1987). Bruch's membrane age related changes vary by region. *Curr. Eye Res.* **6**, 1211–21.

Okubo, A., Rosa, R. H., Bunce, C. V., Alexander, R. A., Fan, J. T., Bird, A. C. and Luthert, P. J. (1999). The relationships of age changes in retinal pigment epithelium and Bruch's membrane. *Invest. Ophthalmol. Vis. Sci.* **40**, 443–9.

Ozaki, S., Johnson, L. V., Mullins, R. F., Hageman, G. S. and Anderson, D. H. (1999). The human retina and retinal pigment epithelium are abundant sources of vitronectin mRNA. *Biochem. Biophys. Res. Commun.* **258**, 524–9.

Ruiz, A., Brett, P. and Bok, D. (1996). TIMP-3 is expressed in human retinal pigment epithelium. *Biochem. Biophys. Res. Commun.* **226**, 467–74.

Sajithlal, G. B., Pandarinathan, C., Gowri, C. and Chandrakasan, G. (1998). Advanced glycation end products induce crosslinking of collagen in vitro. *Biochem. Biophys. Acta* **1407**, 215–24.

Sarks, S. H. (1976). Ageing and degeneration in the macular region: a clinico-pathological study. *Br. J. Ophthalmol.* **60**, 324–41.

Schramm, M., Falkai, P., Tepest, R., Schneider-Axmann, T., Przkora, R., Waha, A., Pietsch, T., Bonte, W. and Bayer, T. A. (1999). Stability of RNA transcripts in post-mortem psychiatric brains. *J. Neural. Transm.* **106**, 329–35.

Sethi, C. S., Bailey, T. A., Luthert, P. J. and Chong, N. H. V. (2000). Matrix metalloproteinase biology applied to vitroretinal disorders. *Br. J. Ophthalmol.* **84**, 654–66.

Smith, M. R., Kung, H. F., Durum, S. K., Colburn, N. H. and Sun, Y. (1997). TIMP-3 induces cell death by stabilizing TNF-alpha receptors on the surface of human colon carcinoma cells. *Cytokine* **9**, 770–80.

Tezuka, M., Koyama, N., Morisaki, N., Salto, Y., Yoshida, S., Araki, N. and Horiuchi, S. (1993). Angiogenic effects of enhanced glycation end products of the maillard reaction on cultured human umbilical chord vein endothelial cells. *Biochem. Biophys. Res. Commun.* **193**, 674–80.

Tong, D., Schneeberger, C., Leodolter, S. and Zeillinger, R. (1997). Quantitative determination of gene expression by competitive reverse transcription–polymerase chain reaction in degraded RNA samples. *Anal. Biochem.* **251**, 173–7.

Van der Schaft, T. L., Mooy, C. M., de Bruijn, W. C., Oron, F. G., Mulder, P. G. and de Jong, P. T. (1992). Histologic features of the early stages of age related macular degeneration. A statistical analysis. *Ophthalmology* **99**, 278–86.

Vranka, J. A., Johnson, E., Zhu, X., Shepardson, A., Alexander, J. P., Bradley, J. M. B., Wirtz, M. K., Weleber, R. G., Klein, M. L. and Ascott, T. S. (1997). Discrete expression and distribution pattern of TIMP-3 in the human retina and choroid. *Curr. Eye Res.* **16**, 102–10.

Weber, B. H. F., Vogt, G., Pruett, R. C., Stohr, H. and Felbor, U. (1994). Mutations in the tissue inhibitor of metalloproteinase-3 (TIMP-3) in patients with Sorsby's fundus dystrophy. *Nat. Genet.* **8**, 352–6.

Yamagishi, S., Hsu, C. C., Taniguchi, M., Harada, S. L., Yamamoto, Y., Ohsawa, K. S., Kobayashi, K. and Yamamoto, H. (1996). Receptor mediated toxicity to pericytes of advanced glycation end products. *Biochem. Biophys. Res. Commun.* **213**, 618–87.

Yan, S. D., Schmidt, A. M., Anderson, G. M., Zhang, J., Brett, J., Zou, Y. S., Pinsky, D. and Stern, D. (1994). Enhanced cellular oxidant stress by the interaction of the advanced glycation endproducts with their receptors/binding proteins. *J. Biol. Chem.* **269**, 9889–97.

Zeng, Y., Rosborough, R. C., Li, Y., Gupta, A. R. and Bennett, J. (1998). Temporal and spatial regulation of gene expression mediated by the promoter for the human tissue inhibitor of metalloproteinases-3 (TIMP-3)-encoding gene. *Dev. Dyn.* **211**, 228–37.

Zhang, J., Desai, M., Ozanne, S. E., Doherty, C., Hales, C. N. and Byrne, C. D. (1997). Two variants of quantitative reverse transcriptase PCR used to show differential expression of alpha-, beta- and gamma-fibrinogen genes in rat liver lobes. *Biochem. J.* **321**, 769–75.